AWARD NUMBER: W81XWH-17-2-0015

TITLE: Real-Time Detection of Cellular Respiratory Biomarkers of Early-Stage Infections Using Terahertz Sensing

PRINCIPAL INVESTIGATOR: Ivan Medvedev

CONTRACTING ORGANIZATION: Wright State University
Datyon, OH 45435

REPORT DATE: May 31th, 2019

TYPE OF REPORT: Annual

PREPARED FOR: U.S. Army Medical Research and Materiel Command
Fort Detrick, Maryland 21702-5012

REPORT DOCUMENTATION PAGE

Form Approved
OMB No. 0704-0188

1. REPORT DATE	**2. REPORT TYPE**	**3. DATES COVERED**
5/31/2019	Annual	1 MAY 2018 – 30 Apr 2019

4. TITLE AND SUBTITLE
Real-Time Detection of Cellular Respiratory Biomarkers of Early-Stage Infections Using Terahertz Sensing

5a. CONTRACT NUMBER
W81XWH-17-2-0015

5b. GRANT NUMBER

5c. PROGRAM ELEMENT NUMBER

6. AUTHOR(S)
Ivan Medvedev (PI), Katherine Excoffon (co-PI), Jennifer Martin (co-PI)

E-Mail: ivan.medvedev@wright.edu

5d. PROJECT NUMBER

5e. TASK NUMBER

5f. WORK UNIT NUMBER

7. PERFORMING ORGANIZATION NAME(S) AND ADDRESS(ES)

Wright State University
Datyon, OH 45435

8. PERFORMING ORGANIZATION REPORT NUMBER

9. SPONSORING / MONITORING AGENCY NAME(S) AND ADDRESS(ES)

U.S. Army Medical Research and Materiel Command
Fort Detrick, Maryland 21702-5012

10. SPONSOR/MONITOR'S ACRONYM(S)

11. SPONSOR/MONITOR'S REPORT NUMBER(S)

12. DISTRIBUTION / AVAILABILITY STATEMENT

Approved for Public Release; Distribution Unlimited

13. SUPPLEMENTARY NOTES

14. ABSTRACT
Early detection and prevention of respiratory infections is a critical mission of military and civilian medical facilities. For example, adenoviruses are a major cause of acute respiratory illness in the military. The hypothesis that different types of cells produce unique profiles of respiratory chemicals (gaseous biomarkers) is substantiated by apparent differences in cell-specific metabolic biochemistry. The research team comprised of Drs. Ivan Medvedev (WSU-Physics), Katherine Excoffon (WSU-Biology), and Jennifer Martin (AFRL) is studying the variability of respiratory chemical profiles for a variety of cellular species, as well as a range of metabolic, homeostatic, and infectious conditions. The analysis is done using THz chemical sensing facility at WSU and Gas Chromatography-Mass Spectrometry (GC-MS) facility at AFRL. We are studying variability of respiration associated with viral infections (such as adenovirus). We are studying the effects of variability of cellular metabolism in response to varying concentrations of glucose, insulin, melatonin, and cortisol intended to simulate a range of cellular stress conditions. An exhaustive range of respiratory biomarkers from cellular models will be collected to create biomarker libraries and investigate the feasibility of using this information for pre-symptomatic detection of related pathologies, unadulterated by competing bio-processes in human body.

15. SUBJECT TERMS
Adenovirus, Virus, Infection, Cellular, Metabolism, Bio-markers, Terahertz, Spectroscopy, Breath, Analysis

16. SECURITY CLASSIFICATION OF:			**17. LIMITATION OF ABSTRACT**	**18. NUMBER OF PAGES**	**19a. NAME OF RESPONSIBLE PERSON**
a. REPORT	**b. ABSTRACT**	**c. THIS PAGE**			USAMRMC
Unclassified	Unclassified	Unclassified	Unclassified	42	**19b. TELEPHONE NUMBER** *(include area code)* 9

Table of Contents

1. **INTRODUCTION:**

Early detection and prevention of respiratory infections is a critical mission of military and civilian medical facilities. For example, adenoviruses are a major cause of acute respiratory illness in the military. The hypothesis that different types of cells produce unique profiles of respiratory chemicals (gaseous biomarkers) is substantiated by apparent differences in cell-specific metabolic biochemistry. We have recently demonstrated the use of THz chemical sensors in detecting chemicals produced by cell cultures in a well-controlled laboratory environment, thus, providing the experimental basis for investigation of this hypothesis. The research team comprised of Drs. Ivan Medvedev (WSU-Physics), Katherine Excoffon (WSU-Biology), and Jennifer Martin (AFRL) is studying the variability of respiratory chemical profiles for a variety of cellular species, as well as a range of metabolic, homeostatic, and infectious conditions. The analysis is done using THz chemical sensing facility at WSU and Gas Chromatography-Mass Spectrometry (GC-MS) facility at AFRL. To identify tissue specific respiratory bio-markers we are studying cellular respiration of the following normal human cell types: lung, liver. Liver cells will be used for baseline comparison. We are studying variability of respiration associated with viral infections (such as adenovirus). We are studying the effects of variability of cellular metabolism in response to varying concentrations of glucose, insulin, melatonin, and cortisol intended to simulate a range of cellular stress conditions. An exhaustive range of respiratory biomarkers from cellular models will be collected to create biomarker libraries and investigate the feasibility of using this information for pre-symptomatic detection of related pathologies, unadulterated by competing biochemical processes in the human body.

2. **KEYWORDS:** Adenovirus, Virus, Infection, Cellular, Metabolism, Bio-markers, Terahertz, Spectroscopy, Breath, Analysis

3. **ACCOMPLISHMENTS:**

- **What were the major goals of the project?**

The main objective of this research program is to determine if Adenovirus infections cause detectable changes in gaseous metabolites produced by in-vitro cell cultures. The quantitative analysis of gaseous metabolites is performed using complementary Terahertz and GC-MS sensing approaches.

This objective is being reached through the following three major tasks.

Major Task 1: To grow primary airway epithelia and liver cell and collection of related Respiratory Volatile Organic Compounds

Major Task 2: Collect all relevant Terahertz spectral libraries

Major Task 3: To infect airway epithelia with adenovirus and identify unique VOC bio-signature

- **What was accomplished under these goals?**

The list of major achievements during the second year (13-24 months) of the research program:

1. Seven runs of human primary epithelial cell growth (each lasting 4-6 weeks) have been conducted. Three runs had to be terminated due to bacterial contamination. Four runs were successful and allowed us to study gaseous metabolic biomarkers of adenovirus infections with THz and GC-MS methods.
2. In Year 1 we tentatively determined that primary epithelial cell gaseous metabolites manifested systematic trends in ethanol and acetaldehyde concentrations associated with adenovirus infection. Year 1 results shown in Figure 4 exhibit rather high concentration of ethanol (~1 ppm), which was traced in Year 2 to a contamination associated with the use of ethanol as a cleaning agent in the incubation facility. In year 2 we took extra precautions to minimize this contamination. All cell cultures were handled in a dedicated fume hood with hydrogen peroxide used as a cleaning agent.
3. Four successfully grown cell cultures we infected with adenovirus. These are referred to as Run 1, 2, 3, and 4 in what follows. The multiplicity of infection used in Year 2 runs was increased to 100 from 10 used in Year 1.
4. To better differentiate gaseous metabolites associated with viral infections we concurrently sampled infected and control cells to look for biomarkers of adenovirus infections.
5. Gaseous metabolites of Runs 1-4 were studied with THz sensing.
6. Gaseous metabolites of Run 2 for infected and control cells at 48 hours were analyzed with GC-MS instruments at AFRL chemical sensing facility (Table 1, Figures 11-14).
7. Gaseous metabolites of Run 4 for infected cells were analyzed with GC-MS instruments at AFRL chemical sensing facility. Six samples were studied: 1. Pre-infected cells; 2. Pre-infected media; 3. 4-hours after infection; 4. 24-hours after infection; 5. 48-hours after infection; 6. 72-hours after infection.
8. THz analyses of gaseous metabolites reveal systematic decrease of ethanol and acetaldehyde concentrations along the timeline of the experiment. Both control and infected cells manifest this effect. The initial concentration of ethanol and acetaldehyde is thought to be present in the cell nutritional media. The concentration of ethanol and acetaldehyde is gradually decreasing (Figure 8) due to evaporation and possible metabolic consumption/production by cells. We detected a slight difference between concentration decay time constant for ethanol and acetaldehyde between control and infected cells (Figure 10). The small margin of variance can be due to

metabolic differences between control and infected cells, but the magnitude of the difference does not allow us to state with confidence that ethanol and acetaldehyde can be used as biomarkers of viral infection.

9. GC-MS analyses for Runs 2 and 4 revealed several chemicals whose concentrations manifest patterns systematic with adenovirus infection (Figures 11-14, Table 1).
10. We are currently preparing to conduct several more cell growth sessions followed by infection with adenovirus to further validate the findings presented in this report.

Goals not met in the during the second year (13-24 months) period:

1. Bacterial contaminations during cell growth has limited us to 4 useful cell growths runs in Year 2. We are currently working on conducting several more cell growth sessions.
2. The GC-MS results presented in this report make us optimistic about finding gaseous biomarkers of viral infections and we are looking to further validate these findings.
3. We will work to develop additional THz spectral libraries for the chemicals deemed

A detailed account of our achievements and approaches follows.

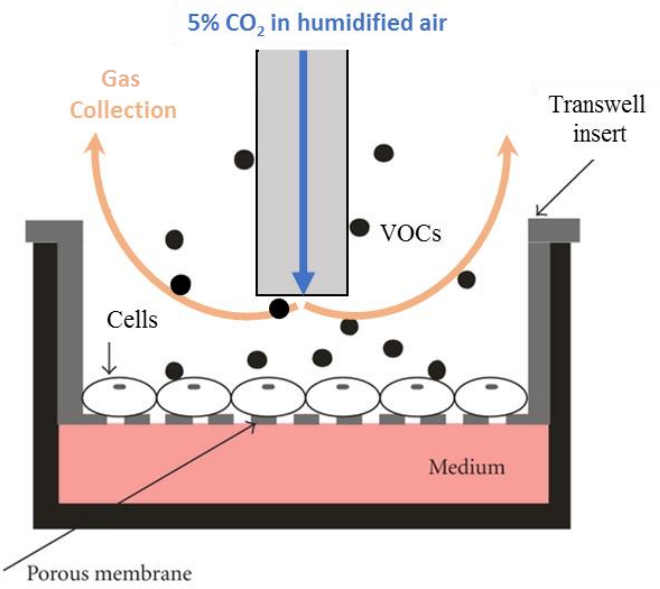

Figure 1. In-vitro THz identification of bio-markers of adenovirus. Organotypic cell cultures grown on a semi-permeable membrane inside a transwell insert and placed at the air-liquid interface (ALI).

Figure 1 shows our approaches to collection of metabolic VOCs from in-vitro cell cultures. In this project we focused on the development of an experimental system capable of collecting metabolic VOCs from

organotypic cell cultures grown at the air-liquid interface (ALI) shown in Figure 1. Cells are grown on top of semi-permeable membrane located at the bottom of a transwell. The transwell is placed on top of the medium. Nutrients from the medium are delivered to cell cultures through the membrane, but the medium surface is not directly exposed to the flow of buffer gas (in our case we use 5% CO_2 in humidified air). When cell cultures are fully polarized permeation of VOCs dissolved in medium is further reduced. This facilitates selective collection of metabolic VOCs from cell cultures. Buffer gas has two roles: 1) it creates the optimum environment for cell wellbeing (for epithelial lung cells it mimics gas composition in human lungs); 2) it transports metabolic VOCs to gas collection hardware. In our case we use Tedlar bags for gas sampling, which are certified by EPA for applications related to sampling and analysis of environmental gas mixtures. Tedlar bags are routinely used in PI's laboratory for collection and THz analysis of human breath, and have proven as a robust method of breath storage, with reliable sample retention up to 72 hours after sample collection.

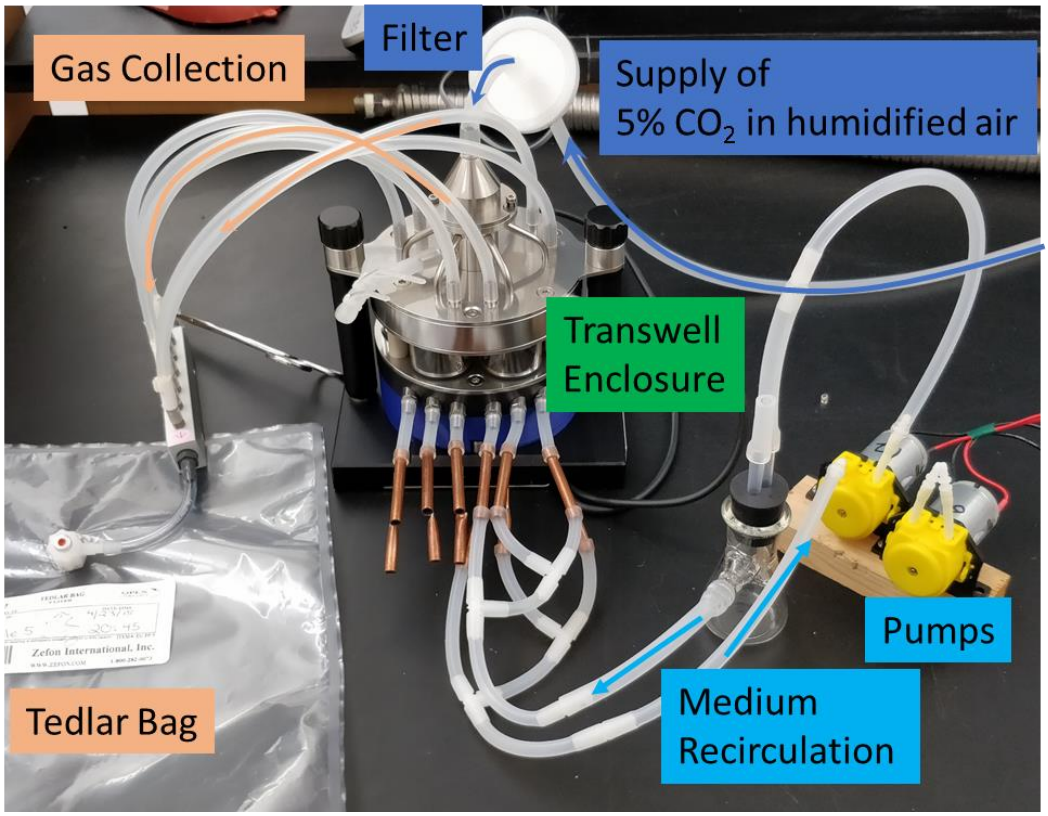

Figure 2. Cell exposure and gas collection system. Cultex exposure system shown in the center, is capable of housing 6 transwell insert. In Blue – A mixture of 5% CO_2 in humidified air flows through Cultex from a pressurized tank at a rate of 10 cc/min controlled by a flow mass controller (not shown in figure). In Orange – Buffer gas enriched with metabolic VOCs is collected into a Tedlar bag. In Cyan - Nutritional

medium is recirculated by a water pump. The set-up shown provides medium recirculation to 3 out 6 enclosures.

Figure 2 shows the modified Cultex cell exposure system procured during this research. Figure 2 shows the custom media recirculation system comprised of 2 peristaltic pumps (shown in yellow), a Buchner flask for medium storage, and custom copper adapters to implement nested tubing for supply and return of media to individual chambers through a single inlet port. A custom base for Cultex system was 3-D printed (blue bottom of Cultex visible in Figures 2 and 3) to accommodate the additional tubing for the recirculation system. Cultex system has proven to be hard to clean and has resulted in bacterial contamination in some of the cell growth/infection runs. Cultex system was used in Run 4 with minimal contamination.

The results presented in this report for Runs 1-3 have been obtained using a custom-built exposure system shown in Figure 3. The system shown in Figure 3 allows us to grow cell cultures with greater surface area. The system consists of an aluminum base with a 4 inch opening for dishes with cell cultures. An air-tight lid has ports for buffer gas supply and return. The system is temperature controlled at 37 degrees Celsius by means of two heaters controlled by two Omega temperature controllers, with temperature readout provided by two thermocouples. The heaters and thermocouples are placed on two sides of the well for better temperature uniformity.

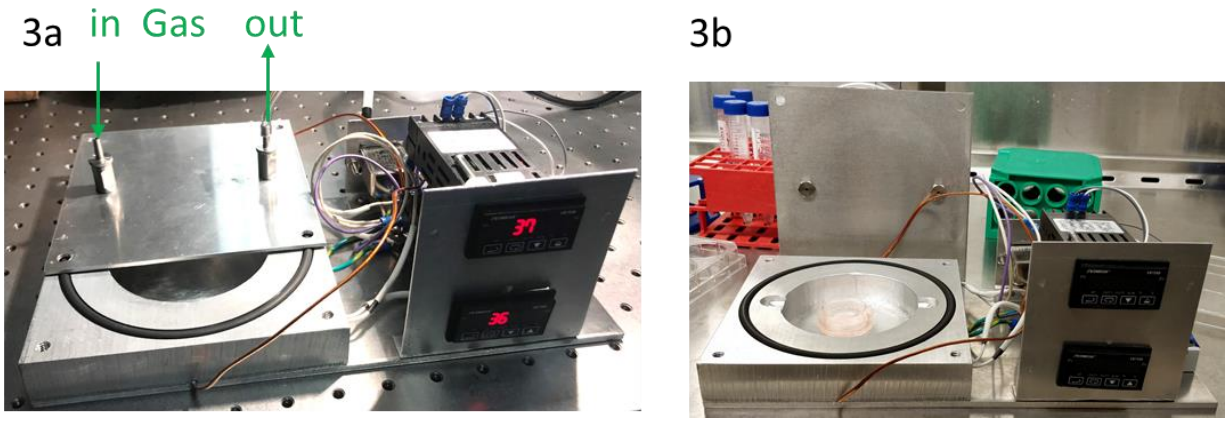

Figure 3. Custom bio-containment/exposure system designed to collect gaseous VOCs from cell cultures. 3a - Bio-containment/exposure system is temperature stabilized at 37°C. 4b - shows dish containing a 2" transwell with medium.

The results presented below for Runs 1-3 were obtained with cells placed into a 2" transwell inside the custom exposure system shown in Figure 3. The cells were grown on a semi-permeable membrane which provided facilitated medium isolation from the buffer gas stream.

Gas chromatography mass spectrometry (GC-MS)

All sorbent tubes were thermally desorbed on a Markes International TD-100 thermal desorber and analyzed on a Trace Ultra-ISQ gas chromatograph in line with a single quadraple mass spectrometer (Thermo Scientific, Waltham, MA). Thermal desorption and GC-MS analysis of sample tubes were conducted as described previously[1]. Briefly, thermal desorption was carried out at 310 °C over 10 min. Trap settings were as follows: flow path temperature 160 °C, trap flow rate 50 ml min^{-1}, trap purge time 1 min, trap low temperature of 25 °C, trap high trap temperature 315 °C, trap heating rate 40 °C s^{-1} and post trap split 3.5 : 1. TO-14 A internal standards, bromocholoromethane, 4-bromofluorobenzene, chlorobenzene-d5, and 1,4-difluorobenzene, were applied automatically to the sorbent tube by the Markes TD-100 prior to thermal desorption (25 ppm, Linde Gas North America, Stewartsville, NJ). GC separations were carried out on a Restek Rxi-624Sil GC column (Bellefonte, PA, 60 m × 0.32 mm ID × 1.80 μm df), with a constant flow of helium (2 ml min^{-1}), over a temperature range of 40 to 240 °C at an increase of 10 °C min^{-1} with a 20 min hold time at the maximum temperature. Mass spectral analysis was carried out via electron impact ionization at 70 eV with an ion source of 275 °C while scanning over a 35–300 m/z range every 0.154 s. Data was acquired using the Thermo Scientific Trace finder EFS software package (v. 3.0). Raw data file conversion from .RAW to .CDF occurred using the File Conversion tool as part of the Xcalibur software package (v. 3.0, Thermo Scientific).

A novel Terahertz gas sensor utilized in this program for chemical analysis has been recently developed in the PI's laboratory with funding from AFOSR[2] . It can detect a wide range of gaseous chemicals at a part per billion to part per trillion level of dilution. The distinct advantage of this technology is the near 'absolute' specificity (extremely low probability of a false alarm) stemming from the highly redundant spectroscopic signatures being used for chemical detection.

[1] Harshman, S.W., Geier, B.A., Fan, M., Rinehardt, S., Watts, B.S., Drummond, L.A., Preti, G., Phillips, J.B., Ott, D.K., and Grigsby, C.C. (2015). "The identification of hypoxia biomarkers from exhaled breath under normobaric conditions". Journal of Breath Research 9, 047103.

[2] "Terahertz Spectroscopic Chemical Sensor for Analysis of Fatigued Human Breath", STTR Phase II, Air Force Research Laboratory, FA8650-16-C-6693

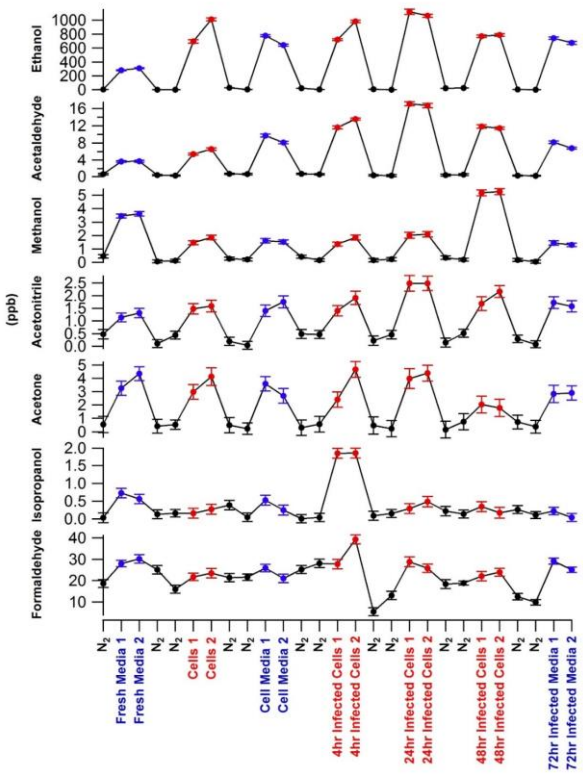

Figure 4. THz quantitative analyses of gaseous samples collected from a sample of healthy Primary human epithelial cell cultures in Year 1. Blue markers correspond to composition of media. Black markers correspond to composition of Tedlar bags filled with pure nitrogen. Red markers correspond to VOCs detected in presence of cell cultures. Consecutive unicolor markers shown correspond to sampling from the same Tedlar bag. All concentrations are measured in parts per billion.

Figure 4 shows Year 1 results from the Year 1 report. Concentrations of gaseous samples produced by primary epithelial cells were determined with THz sensing at WSU. The concentrations of ethanol and acetaldehyde appear to increase and peak at 24h after infection by adenovirus. The high concentration of ethanol (~1 ppm) exceeds the usual abundance of ethanol in human breath, which made us think that the most likely source of ethanol is an external contamination, as ethanol is used as a cleaning agent in Dr. Excoffon's laboratory. In Year 2 we took extra precautions to minimize this contamination. We moved all cell growth and manipulation hardware to a separate hood and started to use hydrogen peroxide as a cleaning agent. This yielded good results, as detected ethanol and acetaldehyde levels dropped significantly. Figures 5,6,7 show much lower levels of ethanol.

In Year 2 we conducted 4 successful cycles of primary human epithelial cell growth and infection referred to as Runs 1-4 in what follows. For Runs 1-3 gaseous metabolites were collected using custom

biocontainment/exposure system shown in Figure 3. For Run 4 gaseous metabolites were collected using Cultex system shown in Figure 4.

The growth of primary human airway requires feeder fibroblast irradiated cells and a unique cocktail of nutrients. The production of sufficient number of feeder fibroblasts and primary human airway epithelial cells requires 4-6 weeks for each run. At that time primary cells can be seeded in transwells as described below and polarized for a minimum of 7 days prior to experiment.

For Runs 1-3 three million primary human airway epithelial cells from healthy donors were seeded onto transwells (3 cm diameter, 0.4 um pore size). Cells were allowed to polarize over 7-14 days by incubation with polarization medium (1:1 mix of Dulbecco's modified Eagle's medium (DMEM) and F12 medium, 2% Ultroser G serum substitute, 1% penicillin-streptomycin) on the basolateral surface. Medium was changed every 2-3 days. This resulted in polarized epithelia containing roughly 1.4 million cells. Epithelia were infected with wild human adenovirus (AdV5), suspended in phosphate buffered saline, at multiplicity of infection of 100 plaque forming units per cell for 2 hours at the apical and basolateral surfaces of the polarized epithelium. During this infection period, baseline gaseous sampling of the medium was performed in order to obtain a profile of the medium for background subtraction. Epithelia were then returned to the medium and gaseous samples were collected from uninfected control epithelia and infected epithelia at 4, 24, 48, and 72 hours after the end of mock (control) or viral exposure. Gaseous sampling of the conditioned media was performed along the timeline of the experiment in order to obtain a profile of the medium post-infection for background subtraction. THz analyses of gaseous samples for control and infected cell/media are shown in Figures 5,6, and 7.

Figures 5,6 and 7 show concentrations ethanol, acetaldehyde, acetone, methanol, methyl cyanide (also known as acetonitrile), isopropanol, n-propanol, and formaldehyde determined with THz sensing. For each time point we measured gaseous dilutions for cells and media in which cell resided (conditioned media). For conditioned media we removed the cells and collected gaseous samples evaporated by the media itself in absence of cell cultures.

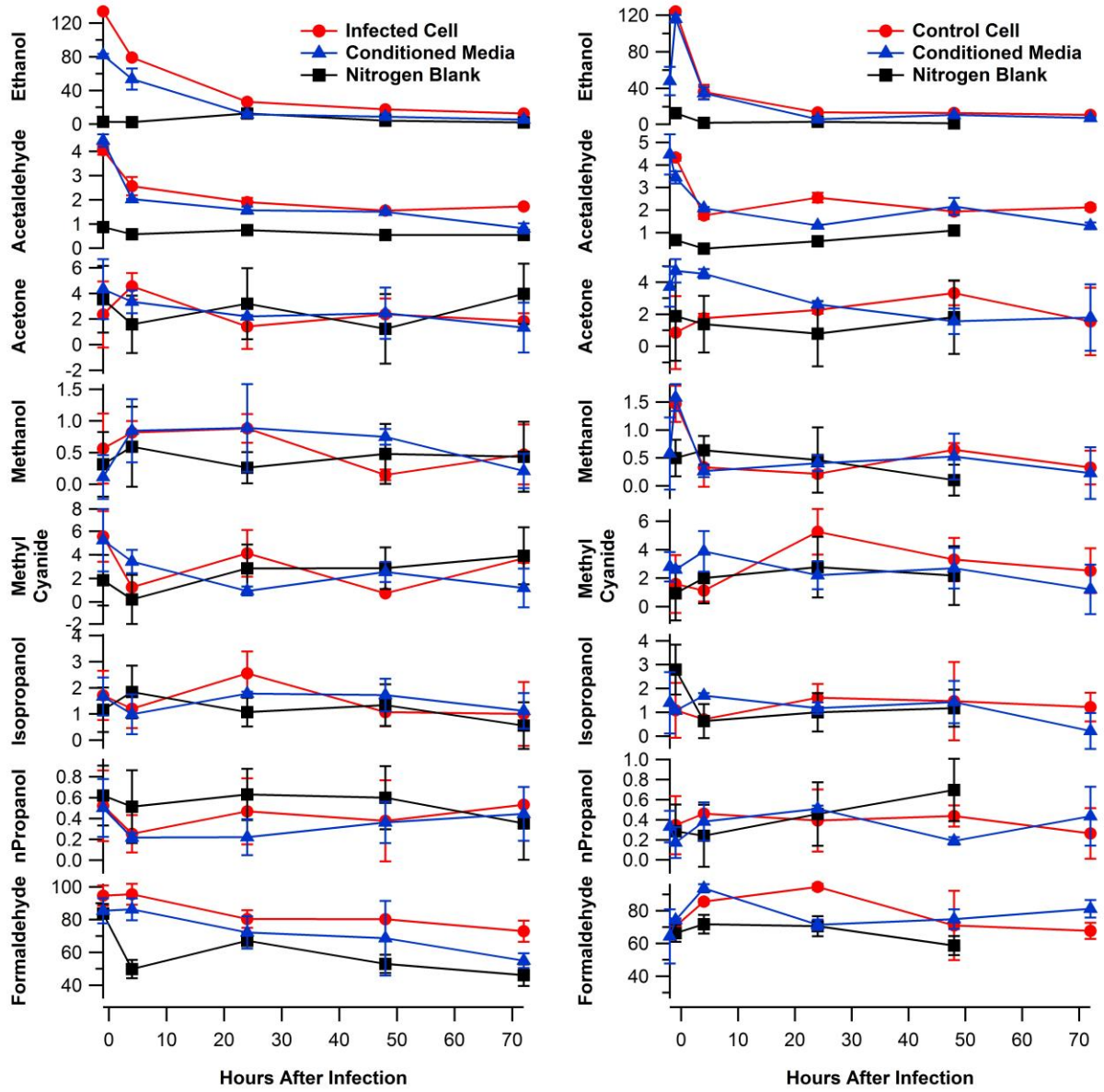

Figure 5. Gaseous metabolite concentrations determined with THz sensing during Run1. Gaseous sample were collected using custom bio-containment/exposure system shown in Figure 3. Gaseous dilutions for Control (right) and Infected (left) cell, Conditioned Media (blue) and Pure Nitrogen Without cells or media (black) are shown in part per billion. Ethanol and Acetaldehyde initial concentrations show gradual reduction due to either evaporation or metabolic consumption. Other chemicals do not show any significant pattern.

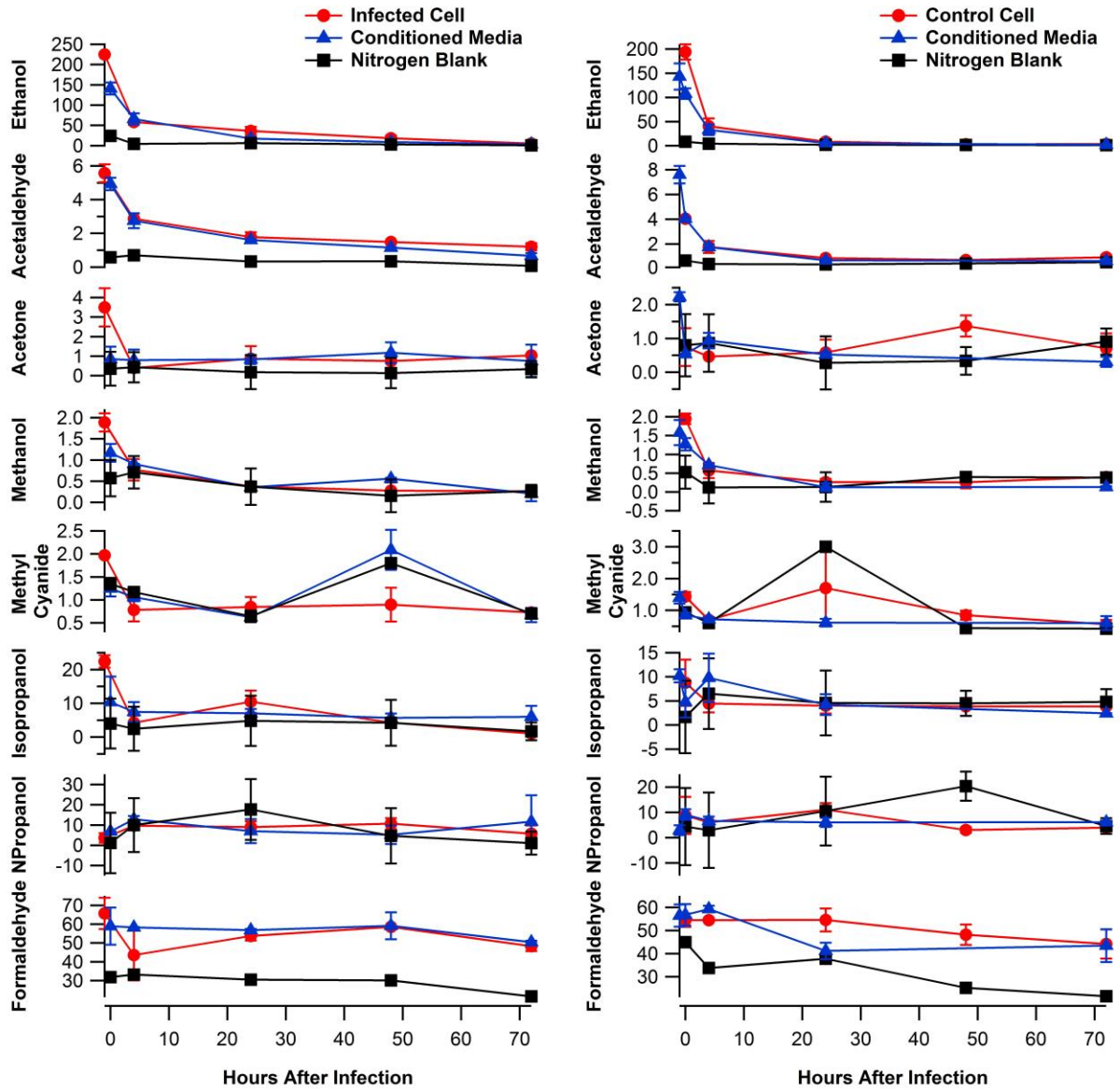

Figure 6. Gaseous metabolite concentrations determined with THz sensing during Run 2. Gaseous sample were collected using custom bio-containment/exposure system shown in Figure 3. Gaseous dilutions for Control (right) and Infected (left) cell, Conditioned Media (blue) and Pure Nitrogen Without cells or media (black) are shown in part per billion. Ethanol and Acetaldehyde initial concentrations show gradual reduction due to either evaporation or metabolic consumption. Other chemicals do not show any significant pattern.

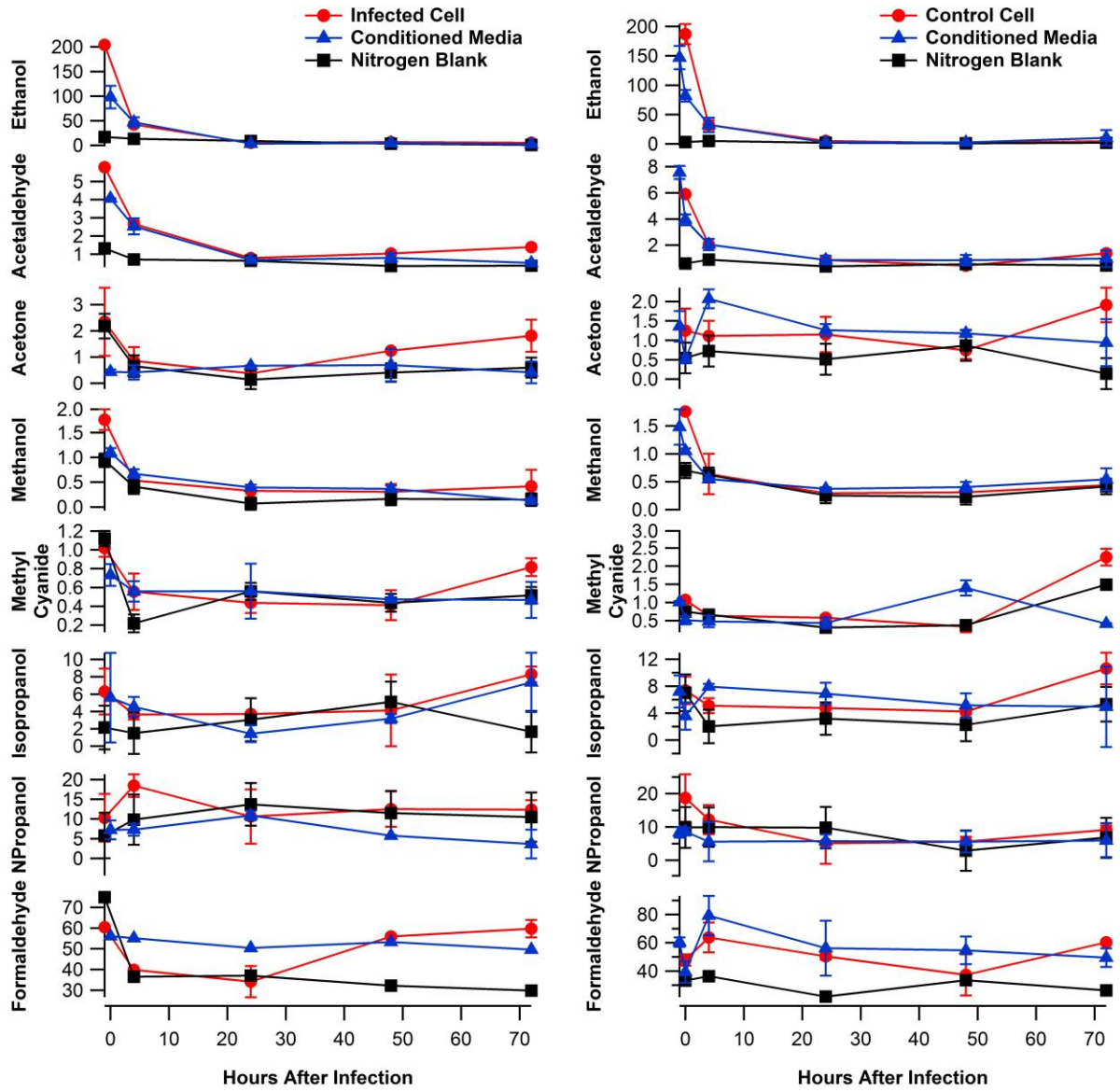

Figure 7. Gaseous metabolite concentrations determined with THz sensing during Run 3. Gaseous sample were collected using custom bio-containment/exposure system shown in Figure 3. Gaseous dilutions for Control (right) and Infected (left) cell, Conditioned Media (blue) and Pure Nitrogen Without cells or media (black) are shown in part per billion. Ethanol and Acetaldehyde initial concentrations show gradual reduction due to either evaporation or metabolic consumption. Other chemicals do not show any significant pattern.

In Runs 1-3 ethanol and acetaldehyde show systematic reduction in dilution along the timeline of the experiment. The initial abundances of these chemicals are most likely due to their presence in nutritional media in trace amounts. Other chemicals show no prominent patterns. To further investigate the patterns of ethanol and acetaldehyde we fitted their concentration to exponential decay equation ($A\,e^{-t/\tau}$, where τ is a decay constant). Excessive scatter in acetaldehyde Run-1 control set did not allow us to get a good fit

of this data. Figure 8 shows the fitting results while Figure 9 show the graphs of decay constants

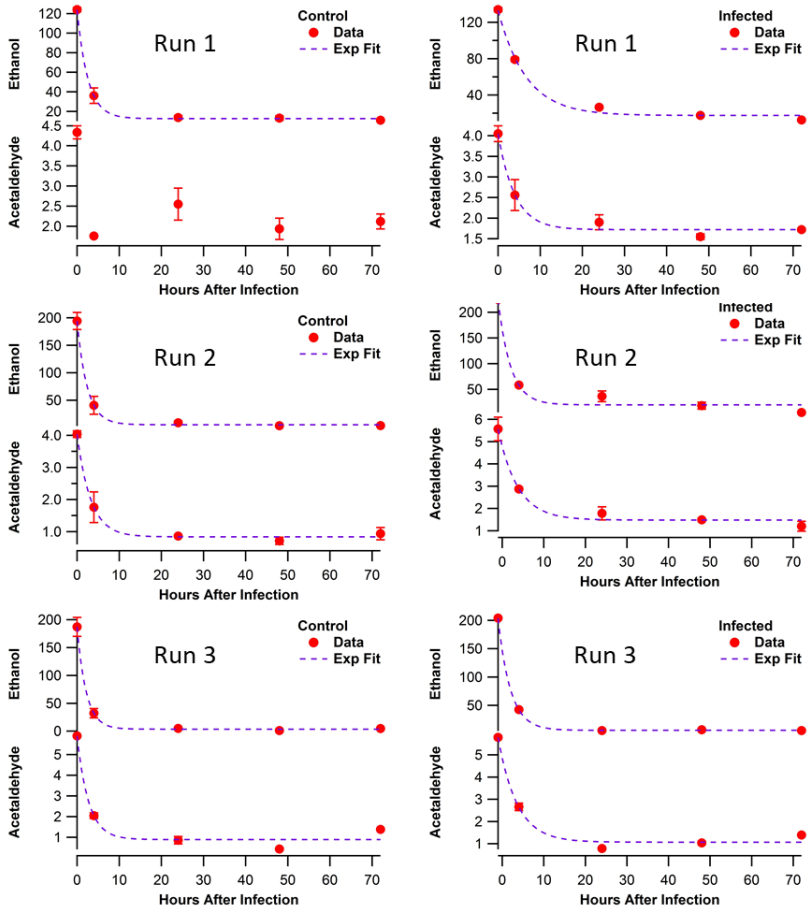

Figure 8. Fitting of ethanol and acetaldehyde concentrations (red) for Runs 1-3 to exponential decay equation. The fitted curves are shown in blue dashed lines. Infected cells exhibit consistently high decay constants.

for ethanol and acetaldehyde. The control (red trace in Figure 9) shown systematically lower decay constant than infected cells (green trace in Figure 9). While the decay itself is most likely due to evaporation, the systematic differences in decay constant shown in Figure 9 can be an indication of metabolic differences between infected and control cells and deserve further investigation.

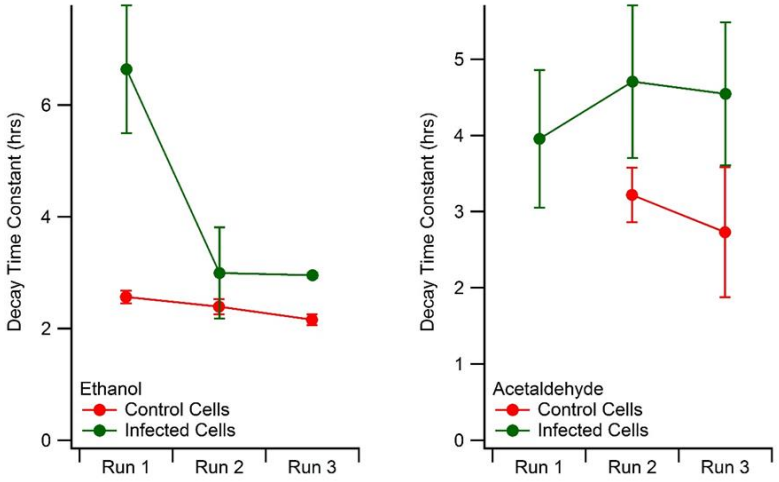

Figure 9. Decay time constants (τ) for ethanol (left) and acetaldehyde (right) dilutions determined with THz sensing. Control cells (red) exhibits systematically lower decay constant than infected cells (green).

For Run 4 one million primary human airway epithelial cells from healthy donors were seeded onto transwells (0.6 cm diameter, 0.4 um pore size). Cells were allowed to polarize over 7 days by incubation with polarization medium (1:1 mix of Dulbecco's modified Eagle's medium (DMEM) and F12 medium, 2% Ultroser G serum substitute, 1% penicillin-streptomycin) on the basolateral surface. Medium was changed every 2-3 days. This resulted in polarized epithelia containing roughly .8 million cells. Epithelia were infected with wild human adenovirus (AdV5), suspended in phosphate buffered saline, at multiplicity of infection of 100 plaque forming units per cell for 2 hours at the apical and basolateral surfaces of the polarized epithelium. During this infection period, baseline gaseous sampling of the medium was performed in order to obtain a profile of the medium for background subtraction. Epithelia were then returned to the medium and gaseous samples were collected from uninfected control epithelia and infected epithelia 4, 24, and 48 hours after the end of mock (control) or viral exposure. Gaseous sampling of the conditioned media was performed along the timeline of the experiment in order to obtain a profile of the medium post-infection for background subtraction. THz analyses of gaseous samples for control and infected cell/media are shown in Figure 10.

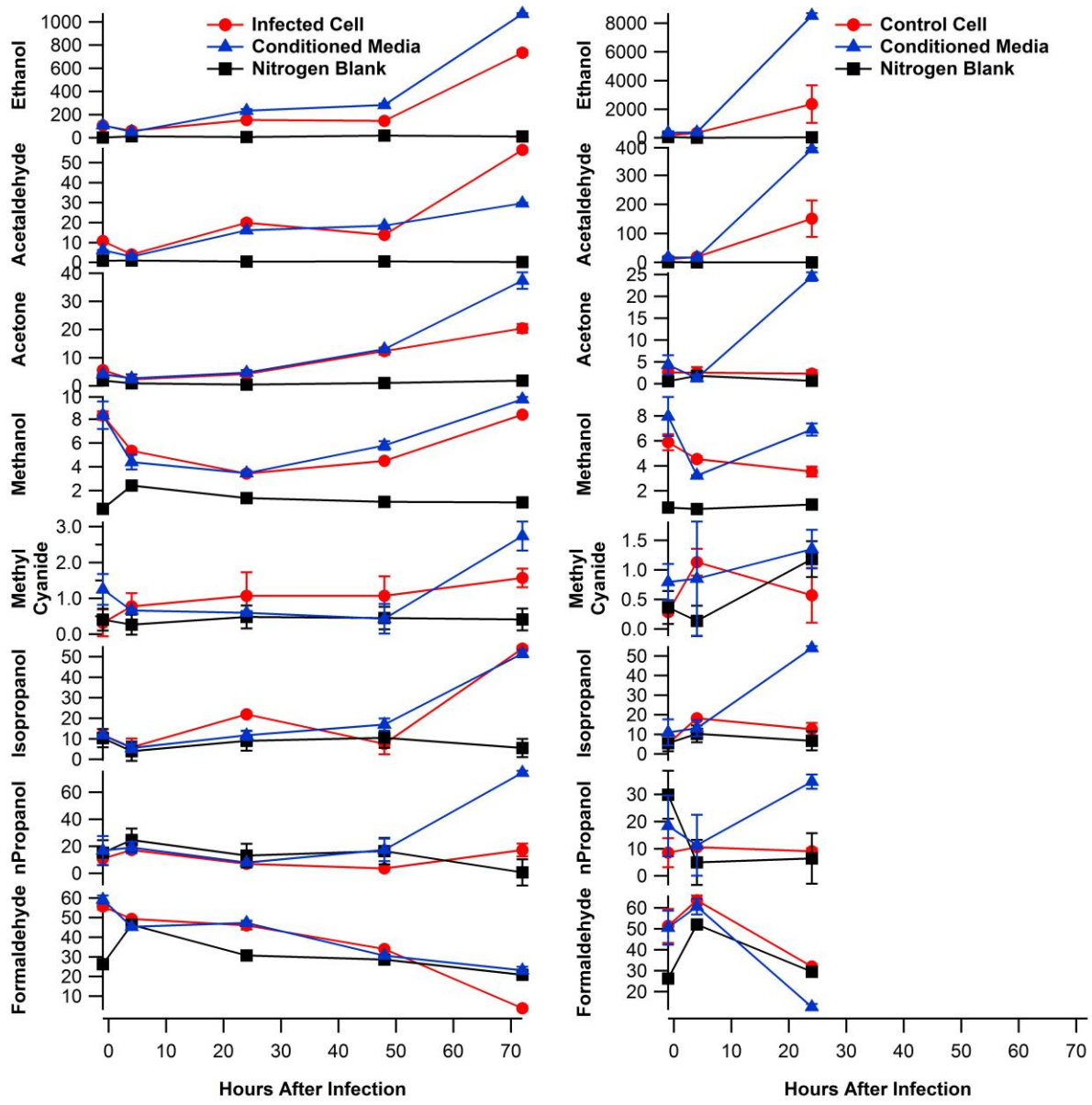

Figure 10. Gaseous metabolite concentrations determined with THz sensing during Run 3. Gaseous sample were collected using Cultex bio-containment/exposure system shown in Figure 2. Gaseous dilutions for Control (right) and Infected (left) cell, Conditioned Media (blue) and Pure Nitrogen Without cells or media (black) are shown in part per billion.

Figure 10 shows THz analyses of gaseous samples collected during Run 4, which was done on Cultex exposure system. Notably the concentrations of ethanol, acetaldehyde, acetone, methanol, methyl cyanide, and iso-propanol all appear to increase during infected cell run. No noticeable contamination was noticed during infected run, but the control cell run had to be abandoned after 24 hours due to obvious bacterial contamination of the control cell culture. The bacterial contamination most likely started during the infected

cell run, which was done first, and got rather prominent during the control cell run despite our efforts to clean the Cultex system with hydrogen peroxide. Despite this we think the GC-MS data collected during Run 4 (see below) provides valuable insight into the gaseous metabolite of viral infection, as the bacterial contamination did not manifest itself up until 48 hours after the infection.

The GC-MS analyses were conducted at AFRL using the state-of-the-art hardware described earlier. Instead of Tedlar bags, the gaseous metabolites were directly loaded onto sorbent tubes containing Tenax sorbent material. A total of 0.5L of gas was drawn through sorbent tubes for each collection. For Run 2 we sampled gas at 48 hour mark for control and infected (labeled T1 and T2 in Table 1). For Run 4 we collected 6 samples: T1 – pre-infected cells (right before infection), T2 – pre-infected media (media conditioned by cell right before infection), T3 – 4 hours after infection, T4 – 24 hour after infection, T5 – 48 hours after infection, T6 – 72 hours after infection. Table 1 summarizes the results of GC-MS analyses and provides chemical name, retention time in minutes (time of sample evolution from the gas-chromatography column), chemical dilutions and associated probabilities of identification. GC-MS analyses were run in a tentative identification mode, when chemicals are identified by fits against libraries. The software determines the match probability which needs to be used as guidance in determining the correctness of the measurement. We present Table 1 in its entirety, but highlight few chemicals (Figures 11, 12, 13, 14 and bold green font in Table 1) that exhibit prominent patterns that can be caused by the introduction of viral infection.

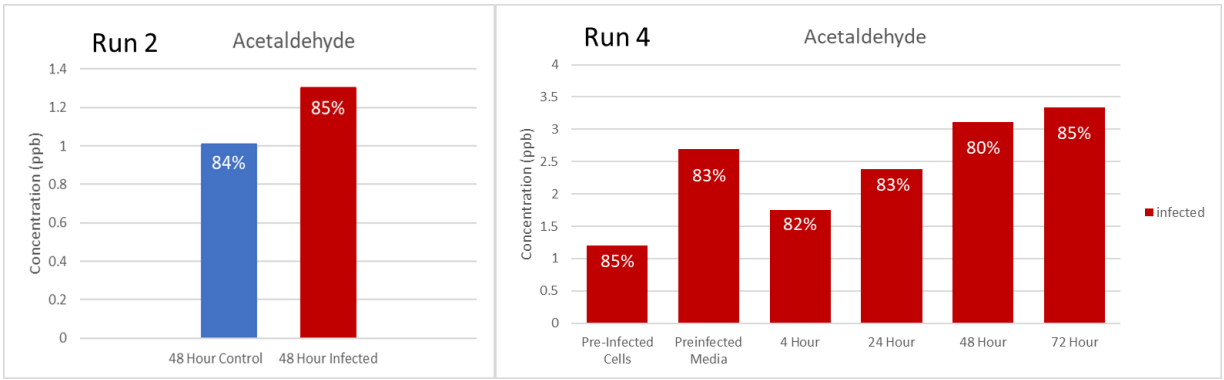

Figure 11. Detection of acetaldehyde with GC-MS. Run 2 measurements of control and infected metabolites at 48 hours are presented in the left pane, while Run 4 data represented on the right. Each bar is labeled with corresponding “Match Probability”.

Figure 11 shows concentrations of acetaldehyde detected in Runs 2 and 4. In both cases THz sensing returns a higher value of acetaldehyde dilution, which speaks for better retention of the analyte in THz

measurement. Notably, ethanol was only detected only in T6 for Run 4 with GC-MS (Table 1), which is emblematic of THz sensor ability to detect light volatiles such as ethanol. Concentration of acetaldehyde increases through Run 4 which tracks well the THz measurements shown in Figure 10. The rise of acetaldehyde (not detected in Runs 1-3) is most likely due to the onset of bacterial infection in the Cultex system, that became prominent during the control run (Figure 10).

Through analysis of data presented in Table 1 we identified several chemicals that could be linked to the onset of viral infections.

Figure 12 shows a rise in concentration of Caprolactam detected with GC-MS in Run 4. No Caprolactam was detected in Run 2. Notably Caprolactam was identified as a possible biomarker of lung cancer in a publication by Wang et al.[3]. Caprolactam "$(CH_2)_5C(O)NH$" is a good candidate for THz detection, with detection at a part per billion level of dilution.

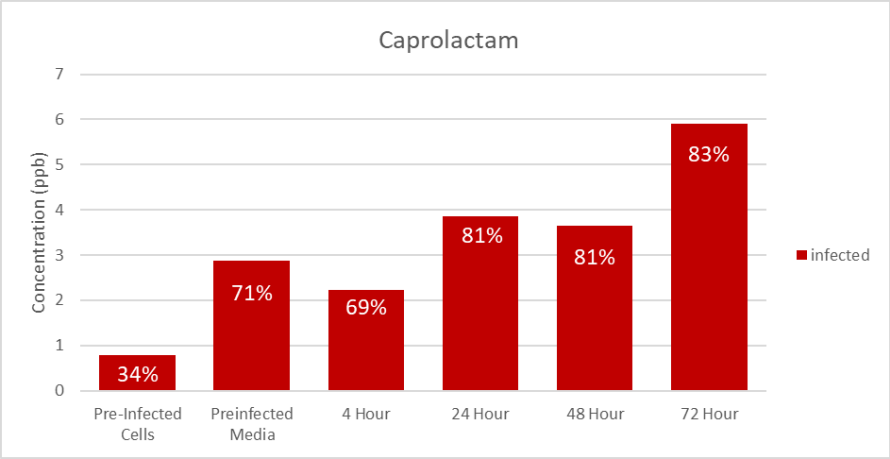

Figure 12. Detection of Caprolactam with GC-MS in Run 4. Each bar is labeled with corresponding "Match Probability".

Figure 13 shows a rise in concentration of 1,2-Benzisothiazole detected with GC-MS in Run 4. No 1,2-Benzisothiazole was detected in Run 2. 1,2-Benzisothiazole "C_7H_5NS" is a good candidate for THz detection, with detection at a part per billion level of dilution.

Figure 14 shows a rise in concentration of acetophenone detected with GC-MS in Run 4. In Run 2 acetophenone was detected at slightly higher concentration in infected cells a 48h mark. The fact that it was present in 48-hour control in Run 2 makes it a less likely candidate as a biomarker of viral infection. Acetophenone "$C_6H_5CCH_3$" is a good candidate for THz detection, with detection at a part per billion level

[3] Wang, C., Dong, R., Wang, X., Lian, A., Chi, C., Ke, C., Guo, L., Liu, S., Zhao, W., Xu, G., and Li, E. (2014). "Exhaled volatile organic compounds as lung cancer biomarkers during one-lung ventilation". Scientific reports 4, 7312.

of dilution.

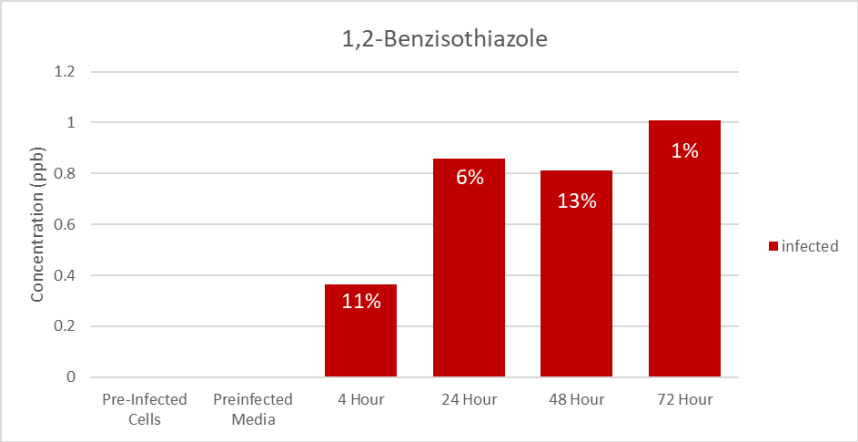

Figure 13. Detection of 1,2-Benzisothiazole with GC-MS in Run 4. Each bar is labeled with corresponding "Match Probability".

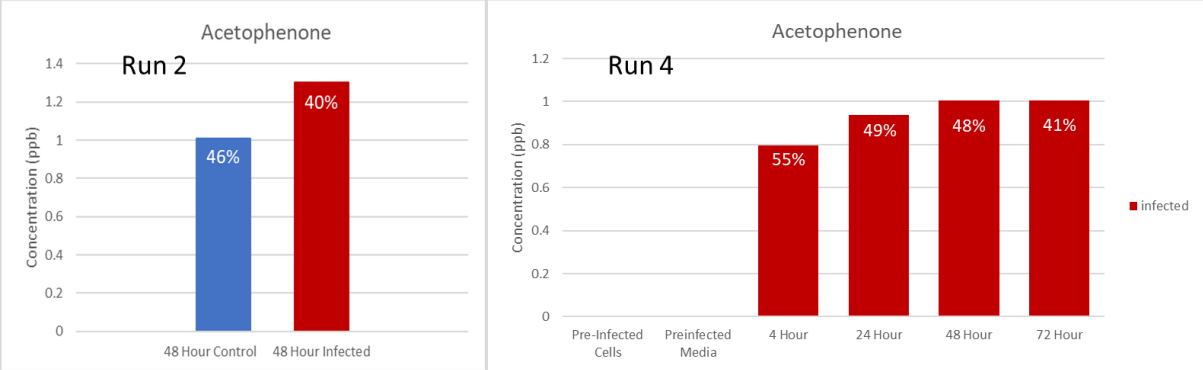

Figure 14. Detection of Acetophenone with GC-MS. Run 2 measurements of control and infected metabolites at 48 hours are presented in the left pane, while Run 4 data represented on the right. Each bar is labeled with corresponding "Match Probability".

2-Butene was detected by GC-MS in 48-hour and 72-hour samples. 2-Butene "C_4H_8" exists in two conformations (cis and trans) and is a very good candidate for detection at a part per billion level of dilution. Ethanol, acetonitrile, and 1 -propanol were detected in 72-hour sample and are also detected by THz in all of Run 4 samples. We hypothesize that increases in concentrations for these chemicals are most likely caused by the onset of the bacterial contamination during Run 4.

2-methyl-propanal and 2-methyl-1-butanol were detected in 48-hour and 72-hour samples of Run 4. Both are excellent candidates for THz detection and will be validated in future experiments.

Spiro-1-(cyclohex-2-ene)-2-(5oxabicyclo[2,1,0]pentane) 1,4,2,6,6-pentamethyl were detected in 48-hour and 72-hour samples of Run 4. This molecule is an unlikely candidate for THz detection, but we will monitor

its presence in future experiments.

Table 1. Chemical analyses of gaseous samples from Runs 2 and 4 conducted with GC-MS.

Chemical Name	Retention Time (min)	Concentration (ppb)															
		Run 2				Run 4											
		T1		T2		T1		T2		T3		T4		T5		T6	
		Control 48 h	Match Probability	Infected 48 h	Match Probability	Pre-Infected Cells	Match Probability	Pre-Infected Media	Match Probability	4 h	Match Probability	24 h	Match Probability	48 h	Match Probability	72 h	Match Probability
Carbamic acid, monoammonium salt	3.31	0.42	60%	0.334	57%	0.473	33%	0.739	59%	0.657	59%	0.894	57%			0.565	59%
Carbon dioxide	3.31	0.42	32%	0.334	31%	0.473	57%	0.739	32%	0.657	32%	0.894	31%			0.565	32%
Aminomethanesulfonic Acid	3.79					0.67	4%	1.123	5%	0.939	5%	0.926	5%			1.154	5%
Sulfur dioxide	3.79			0.201	22%	0.67	94%	1.123	89%	0.939	93%	0.926	90%			1.154	92%
L-Alanine, 3-sulfo	3.79			0.201	66%												
1,3-Difluoro-2-propanol	3.8													1.914	12%		
Phosgene	3.8													1.914	2%		
1-Propene, 2- methyl	4.05													0.544	10%	0.52	16%
2-Butene	**4.05**													**0.544**	**47%**	**0.524**	**40%**
Acetaldehyde	**4.22**	**1.223**	**84%**	**1.409**	**85%**	**1.198**	**85%**	**2.696**	**83%**	**1.745**	**82%**	**2.382**	**83%**	**3.106**	**80%**	**3.334**	**85%**
Ethyne,fluoro-	4.22					1.198	0%			1.745	0%						
Ethylene Oxide	4.22	1.223	4%	1.409	5%			2.696	4%			2.382	4%			3.334	4%
Oxiranemethanol (R)	4.22													3.106	3%		
Pentane	5.1			2.932	69%					6.842	73%						
Propane, 1-chloro-2-methyl	5.1									6.842	3%						

Butane, 2-methyl	5.1			2.932	10%															
Ethanol	**5.11**																	**20.17**	**72%**	
Methane, nitroso-	5.11																	20.17	21%	
Acetonitrile	**5.88**																	**0.569**	**52%**	
Methyl Isocyanide	5.88																	0.569	38%	
Cyclobutane methyl-	6.24	0.202	19%																	
2(3H)-Furanone, dihydro-3,4-dimethyl	6.24	0.202	1%																	
Cyclobutane, methyl	6.25			2.152	25%															
Cyclopentane	6.25			2.152	40%															
1-Pentene, 4-methyl-	6.57					0.659	10%	0.364	27%											
Cyanic acid, 2-methylpropyl ester	6.57					0.659	3%	0.364	7%					0.998	3%	0.908	2%			
1-Hexene	6.57									0.396	18%									
Cyclopropane, 1-ethyl-2-methyl	6.57	0.117	14%							0.396	5%									
Propanal, 2-methyl-	6.57													0.998	64%	0.908	65%			
2H-Pyran-2-one, tetrahydro-5,6-dimethyl-trans-	6.57	0.117	1%																	
1-Pentanol	6.69			0.497	24%															
Hydroperoxide, heptyl	6.69			0.497	19%															
1-Propanol	**6.75**																	**0.997**	**91%**	
2,5-Furandione, dihydro-3-methyl	6.75																	0.997	0%	
Cyclobutane, methyl-	6.77	0.196	4%																	
Cyclopropanecarboxaldehye	6.77	0.196	17%																	
Furan, 2-methyl	7.07					0.814	8%													

Disulfide, bis[1-(methylthio)ethyl]	7.08	0.138	1%			0.814	0%	0.655	1%	0.59	1%	0.932	1%	0.652	1%															
Silanol, trimethyl-	7.08	0.138	41%					0.655	65%	0.59	70%	0.932	73%	0.652	70%	0.577	70%													
tert-butyldimethylsilanol	7.08															0.577	5%													
Butanal, 2-ethyl-	7.21							0.468	2%																					
Oxirane, 2,3-dimethyl-, trans-	7.21					0.278	9%																							
1,3-Butanediol (S)-	7.21									0.371	20%			0.375	12%															
Butane, 1-(ethenyloxy)-3-methyl-	7.21									0.371	4%																			
Cyclobutanol	7.21	0.094	13%											0.375	9%															
2-Propanone, 1-cyclopropyl-	7.2															0.484	0%													
Formic Acid ethenyl ester	7.2															0.484	1%													
2-propen-1-ol-2-methyl. Acetate	7.21					0.278	3%																							
4-Methyl-1,3,2-dioxathiene 2-oxide	7.22	0.094	4%					0.468	11%																					
Hexane, 3,3,4,4-tetrafluoro-	7.27	0.225	6%					0.415	2%	0.327	2%																			
Methanesulfonyl azide	7.27	0.225	15%					0.415	11%	0.327	23%																			
2(3H)-Furanone, dihydro-3,4-dimethyl	7.27			0.366	0%																									
Isoxazolidine, 5-ethyl-2,4-dimethyl	7.27			0.366	0%																									
5-[2-(Trimethylsilyl)cycloprop-1-ylidene]cyclopenta-1,3-diene	7.46					0.609	0%																							
N-Acetylethylenediamine	7.46					0.609	0%																							
Acetic acid	7.87	0.527	67%	0.724	32%	2.884	71%	3.062	77%	1.946	77%	2.802	77%	1.604	79%	2.241	75%													
Ammonium Acetate	7.87					2.884	23%	3.062	18%	1.946	17%	2.802	18%	1.604	15%	2.241	19%													
Acetic Acid anhydride with formic acid	7.87	0.5274	16%	0.724	32%																									
Propanoic Acid, 2- (aminooxy)	8.09	0.134	1%																											

1,3-Dioxolane, 2-methyl	8.09	0.134	11%																			
Butanal, 3-methyl-	8.47					2.07	80%	0.61	71%							0.954	74%	0.817	71%			
Pentanal	8.47					2.07	10%	0.61	14%									0.817	15%			
Oxirane, 2,-methyl-2-(1-methylethyl)	8.47															0.954	0%					
1-Propene, 3-propoxy-	8.62															0.378	4%	0.441	7%			
Butanal, 3-methyl-	8.62															0.378	41%	0.441	43%			
d-Leucylglycine	8.82	0.119	4%																			
Hexylamine, N-methyl-N-propyl	8.82	0.119	0%																			
2-Hexene, 5,5,-dimethyl, (Z)-	9.01	0.325	33%	0.532	39%																	
Pentane, 2,2,4-trimethyl-4-nitro	9.01	0.325	45%	0.532	39%																	
1,1-Bis(2-methoxyethyl)hydrazine	9.45					0.214	1%									0.29	3%					
1-Propoxy-3,3-diethyltriazene 2-oxide	9.45					0.214	0%															
Ketone, methyl-2-methyl-1,3-oxothiolan-2-yl	9.45															0.29	0%					
Heptane 3,4,5-trimethyl	10.11			0.236	2%																	
Heptane 2,4,6-trimethyl	10.11			0.236	5%																	
Silane, methyl-	10.18							0.721	3%	0.797	3%											
Silanediol, dimethyl-	10.18							0.721	59%	0.797	63%											
1-Butanol, 2-methyl-	**10.29**															**1.266**	**51%**	**13.731**	**50%**			
1-Butanol, 2-methyl (S)	10.29															1.266	34%	13.731	37%			
Allyl methallyl ether	10.5	0.191	11%	0.184	1%			0.393	5%									0.386	11%			
Hexane, 2-methyl-4-methylene-	10.5	0.191	6%	0.184	13%			0.393	9%									0.386	1%			
3-Methylheptyl acetate	10.5																					

Hexane, 2,4-dimethyl-	10.62	0.391	18%	0.78	25%	0.762	22%	0.673	15%	0.556	22%	0.576	17%	0.583	23%	0.79	33%
Octane	10.62	0.391	49%	0.78	39%	0.762	35%	0.673	52%	0.556	35%	0.576	49%	0.583	37%	0.79	20%
1,1,3,3-Tetramethyl-1,3-bis[(2Z)-p	11.17							0.445	13%			0.738	10%	0.353	12%		
1,3-Diisopropoxy-1,3-dimethyl-1,3-disilacyclobutane	11.17					0.32	16%	0.445	16%	0.32	12%	0.738	34%	0.353	17%		
1,3-Cyclohexadiene, 1,2,3,4,5,6-hexamethyl-	11.17					0.32	4%										
1,3-bis[(2Z)-Hex-2-en-1-yloxy]-1,1,0	11.17									0.32	11%						
Oxetane, 2,4,-dimethyl-trans-	11.19	0.173	6%	0.118	1%												
1,4-Dioxane, 2,5-dimethyl	11.19	0.173	15%	0.118	2%												
1,6:3,4-Dianhydro-2-deoxy-β-d-lyxo-hexopyranose	11.41	0.088	0%	0.107	1%							0.35	0%	0.368	0%		
Cyclobutanol, 2-ethyl-	11.41					0.527	5%	0.562	8%	0.374	9%						
Hexanal	11.41	0.088	38%	0.107	8%	0.527	52%	0.562	44%	0.374	54%	0.35	30%	0.368	39%	0.585	34%
4-Isopropylcyclohexylamine	11.41															0.585	2%
1,4-dioxane-2,4-dimethyl	11.82			0.161	3%												
1,4-Dioxane,2,5-methyl-	11.82	0.109	15%														
N-nitroso-2-methyl-oxazolidine	11.82	0.109	16%	0.161	14%												
Octane,2-methyl	11.92	0.106	11%	0.204	9%												
2,6-Dimethyldecane	11.92	0.106	5%														
Heptane, 2,4,6-trimethyl-	11.92					0.35	6%										
Decane	11.92			0.204	7%	0.35	10%										
Heptane, 2,4,6-trimethyl-	12.61	0.509	15%	0.842	44%	1.259	11%	1.112	11%	0.649	10%	0.854	14%	0.827	11%	1.319	8%
Nonane	12.61	0.509	38%	0.842	12%	1.259	41%	0.385	27%	0.649	35%	0.854	19%	0.827	18%	1.319	13%
3,5-Dimethyl-1,6-heptadien-4-ol	12.84	0.091	0%														

Isoamyl Cyanide	12.84	0.091	6%																			
3-Heptanone	13.11					0.497	0.497	27%														
3-Hexanone, 5-methyl-	13.11					0.497	29%															
2H-1-Benzopyrane, 3,5,6,8a-tetrahy	13.12							0.385		29%												
Edulan II	13.12							0.385		28%												
Heptanal	13.43	0.099	39%			0.587	0.587	66%	0.702	48%	0.467	0.467	43%	0.418	0.418	33%	0.395	0.395	41%	0.7	0.7	45%
Hexanal, 5-methyl-	13.43	0.099	3%			0.587	3%	0.702	4%	0.467	0.467	4%	0.418	0.418	3%	0.395	0.395	3%	0.7	0.7	3%	
Ethanol, 2-butoxy	13.6	0.131	0%																			
Ethylene Glycol Monoisobutyl Ether	13.6	0.131	0%	0.19	2%																	
Trimethyl [4-(1,1,3,3-tetramethylbutyl)phenoxy]silane	13.6	0.131	0%																			
Ethanol, 2-butoxy	13.6			0.19	3%																	
2-Oxo-4-phenyl-6-(4-chloropheny	13.84	1.01	0%	1.303	0%	5.937	5.937	0%	6.096	0%	4.31	4.31	0%	4.787	4.787	0%	4.35	4.35	0%	5.563	5.563	0%
Cyclotetrasiloxane, octamethyl-	13.84	1.01	83%	1.303	81%	5.937	80%	6.096	83%	4.31	4.31	83%	4.787	4.787	82%	4.35	4.35	79%	5.563	5.563	83%	
(2-Methyl-[1,3]dithian-2-yl)phenyl	14.04	0.14	0%	0.231	0%			2.211	0%	1.593	1.593	0%	1.474	1.474	0%	1.356	1.356	0%				
Oxime-, methoxy-phenyl-_	14.04	0.14	28%	0.231	36%			2.211	44%	1.593	1.593	43%	1.474	1.474	45%	1.356	1.356	43%	1.286	1.286	42%	
4-Ethylbenzoic Acid cyclopentyl ester	14.04																		1.286	1.286	2%	
1-Cyclohexyldimethylsilyloxy-3-phenylpropane	14.22					1.158	1.158	0%	1.934	1.934	1.059	1.059	0%			1.275	1.275	0%				
Phenyl-pentamethyl-disiloxane	14.22					1.158	2%	1.934	2%	1.059	1.059	1%	1.402	1.402	3%	1.275	1.275	1%				
Vanillan, tert-butyldimethylsilyl ether	14.22												1.402	1.402	12%							
2-Methoxymandelic acid, ethyl ester, TMS	14.22																		2.103	2.103	0%	
5-Chloro-1,3-dimethyl-1H-pyrazol-4-sulfonic acid, 2-methyl-5-trifluoromethyl-2H-pyrazole-3-yl-ester	14.22																		2.103	2.103	0%	
1,2,4-Benzenetricarboxylic acid, 1, 2-dimethyl ester	14.4							0.907	0%										0.952	0.952	0%	

Cyclotrisiloxane, hexamethyl-	14.4					0.664	18%	0.907	32%	0.65	14%	0.793	27%	0.664	25%	0.952	26%
Trimethyl[4-(1,1,3,3,-tetramethylbutyl)phenoxy]silane	14.4					0.664	0%					0.793	0%	0.664	0%		
Arsenous Acid, tris(trimethylsilyl)	14.4									0.65	49%						
2-methyl-1-tetradecene	14.41	0.102	0%														
2-methyl-n-1-tridecene	14.41	0.102	0%														
3-dodecene (E)	14.41	0.102	0%														
Heptane, 1-(butenyloxy) - (E)	14.41			0.141	3%												
2- Pentane, 1-(butenyloxy) - (E)-	14.41			0.141	0%												
Decane	14.48	0.084	17%														
Undecane, 2,6-dimethyl	14.48	0.084	0%														
Butyrolactone	14.98	0.074	17%							0.364	0%						
Ethanamine, N-ethyl-N- [(1-methyl)]	14.98									0.364	0%						
1,3,6-Trioxa-2-silacyclooctane, 2,2,	14.98							0.455	17%								
1,3-Dioxane, 4,5-dimethyl-	14.98							0.455	0%								
4-Thiepanone,5-hydroxy-3,3,6,6,-	14.98					0.329	2%										
Decane, 2-methyl-	14.98					0.329	0%										
trans-4,5-Epoxynonane	14.98					0.329	0%										
Butanoic Acid, 4-hydroxy	14.98	0.074	20%														
Bicyclo[4.2.0]octa-1,3,5-triene-7,8-dione	15.12											6.631	16%				
Benzenemethanimine	15.12											6.631	20%				
2-Octen-1-ol	15.32					2.698	6%	1.832	4%	1.194	5%			0.792	5%	1.454	4%
Octanal	15.32	0.229	61%	0.225	54%	2.698	67%	1.832	72%	1.194	68%			0.792	68%	1.454	69%

Z-2-Dodecenol	15.32														1.824		0%					
Undecanal	15.32														1.824		5%					
2-Decan-1-ol, (E)	15.32														1.824		5%					
Cyclohexanal, 2,4-dimethyl	15.33				0.225																	
2-Hexanol, 3,4-dimethyl	15.33		0.229																			
Ethanol, 2-[2-(2-ethoxyethoxy)	15.49		0.176		1%																	
Ethanol, -2-(2-ethoxyethoxy)	15.49		0.176		1%		0.461		70%													
1,5-Cyclooctadiene, 1,5-dimethyl-	15.49											0.621		0%		0.542		0%				
Cyclohexene, 1-methyl-5-(1-methylethenyl)-, (R)-	15.49							0.531		10%		0.621		2%		0.542		5%	1.229		0%	
Limonene	15.49							0.531		2%									1.229		0%	
5,1- propenylmethanethiosulfate	15.49				0.461		0%															
Benzene, 1,4-dichloro	15.56				0.173		7%															
Benzene, 1,2-dichloro	15.56				0.173		12%															
2-tert-Butyl-3,4,5,6-tetrahydropyridine	15.79				0.772		0%															
1-Hexanol, 2-ethyl-	15.79		0.633		5%	0.772		13%	1.863		17%	1.716		22%		1.242		15%	2.538		10%		2.176		18%
2-Propyl-1-pentanol	15.79		0.633		2%	0.772		8%	1.863		26%	1.716		14%		1.242		9%	2.538		6%		2.176		18%
5-Methyl-1-heptanol	15.79		0.633		0%																	
1H-Pyrrole-3-carbonitrile	16.06											13.747		0%								
2-Propyn-1-amine, N-2-propynyl-	16.06											13.747		0%								
Phenol	16.06		0.624		45%	0.774		42%	1.048		14%					1.34		23%	1.613		20%		1.066		24%
Phosphonic Acid, (p-hydroxyphenyl)	16.06		0.624		31%	0.774		31%	1.048		13%					1.34		42%	1.613		23%		1.066		27%
2-Hydroxymandelic acid, ethyl ester, di-TMS	16.51					0.173		0%	2.077		0%					1.593		0%	2.284		0%		2.064		0%

4-Hydroxymandelic Acid, ethyl ester, di-TMS	16.51																	1.237	10%	2.064	6%
Benzaldehyde, 2,5-bis[(trimethylsilane)]	16.51					2.077	29%														
4-Trimethylsilyl-9,9-dimethyl-9-sil	16.51									1.593	3%	2.284	3%								
Dicholoracetic Acid, 2-petnadecyl ester	16.51	0.12	0%																		
2-Heptafluorobutyroxydodecane	16.51	0.12	0%																		
3-Heptafluorobutyroxytridecane	16.51	0.12	0%																		
N-Methyl-2-(4-chlorophenyl) eth-2-en-2-yl-1H-benzimidazole	16.51			0.173	0%																
2-Hydroxymandelic Acid, ethyl ester	16.6	0.4	1%																		
2-Hydroxymandelic acid, ethyl ester, di-TMS	16.59			0.597	1%	8.966	1%			4.393	2%	6.128	1%			3.851	1%	5.659	1%		
p-Trimethylsilyloxyphenyl-bis(trim0)	16.59	0.4	7%	0.597	7%	8.966	12%			4.393	11%	6.128	11%			3.851	13%	5.659	11%		
1,3-Dioxolane, 2-heptyl-	16.6							0.9	10%												
1-Propene-1-thiol	16.6							0.9	12%												
Acetophenone	17.03	0.245	46%	0.317	40%					0.796	55%	0.937	49%			1.005	48%	1.007	41%		
1-pentanone, 1-phenyl	17.03									0.796	17%										
1-Hexanone, 5-methyl-1-phenyl	17.03	0.245	1%	0.317	1%							0.937	1%			1.005	1%	1.007	1%		
2-Nonen-1-ol	17.08	0.704	12%	0.526	12%	8.447	10%	4.364	14%	3.842	13%	2.965	12%	1.939	13%	4.065	11%				
Nonanal	17.08	0.704	64%	0.526	59%	8.447	72%	4.364	72%	3.842	68%	2.965	65%	1.939	64%	4.065	65%				
Cyclotetrasiloxane, octamethyl-	17.15											0.738	54%	0.274	43%						
2-Oxo-4-phenyl-6-(4-Chlorophenyl)	17.15											0.738	0%								
3-Ethoxy-1,1,1,5,5,5-hexamethyl-3-(trimethylsiloxy)trisiloxane	17.15													0.274	3%						
1-Undecanol	17.82	0.182	1%	0.137	0%																
3-Dodecene, (E)-	17.82	0.182	2%	0.137	1%																

Hydroxylamine, O-decyl	17.87	0.084	2%	0.098	5%															
2,6-Dimethyldecane	17.87	0.084	1%																	
Decane, 2-methyl	17.87			0.098	2%															
1-Undecanol	18.13					0.463	4%	0.546	6%	0.451	5%	0.405	5%	0.35	3%					
Cyclooctane, methyl-	18.13							0.546	1%	0.451	1%	0.405	1%							
Decane, 3-chloro	18.13					0.463	1%													
2-Methyl-1-Undecanol	18.13													0.35	1%					
1,3-Dioxolane, 4-[[(2-methoxy-4-one)]	18.52					0.267	0%													
9-Octadecanone	18.52					0.267	0%													
Decanal	18.72	0.365	43%			3.435	55%	3.358	50%	2.744	48%	2.078	50%	1.861	46%	3.016	48%			
Undecanal	18.72	0.365	2%	0.311	2%	3.435	2%	3.358	2%	2.744	2%	2.078	2%	1.861	2%	3.016	2%			
Dodecanal	18.72			0.311	6%															
1,3-Butadiene, 1,1,2,3,4,4-hexachloro	18.82			0.149	52%															
Adenosine,(N6)-[3-nitrobenzyl]-4-[N-ethylcarbamyl]-4-dihydroxymethyl-	18.82			0.149	0%															
Pyrazole[3,4-b]pyran-5-carbonitrile-1,4-dihydro-6-amino-4-(2-iodophenyl)-3-methyl	19.13			0.105	13%															
1,2,4-Triazole-3-carboxamide, N-(2,3-dihydro-2-oxo-5-benzimidazolyl)	19.13	0.066	4%	0.105	10%															
2-Isopropyl-5-methyl-6-oxabicyclo [3,1,0] hezane-1-carboxaldehyde	19.13	0.066	0%																	
3-Oxa-6-thia-2,7-disilaoctane, 2,2,7,7-tetramethyl-	19.29	0.313	6%	0.594	9%	0.801	6%	1.244	5%	1.118	5%	1.091	7%	0.999	7%	0.949	5%			
1-Pentamethyldisilyloxyprop-2-en	19.29					0.801	0%									0.949	0%			
2-methyl-1-pentadimethylsiloxyl	19.29									1.118	0%									
Silane, trimethyl[4-(trimethylsilyl)butoxy	19.29	0.313	0%	0.594	0%			1.244	0%			1.091	0%	0.999	0%					
Benzeneacetic acid, α,4-bis[(trimethylsilyl)oxy]-, methyl ester	19.59							0.575	0%			0.533	0%							

Cyclotetrasiloxane, octamethyl-	19.59							0.575	1%					0.553	1%					
1,2-Benzisothiazole	**19.81**	**0.069**	**26%**							**0.365**	**11%**	**0.859**	**6%**	**0.811**	**13%**	**1.008**	**1%**			
Thieno [2,3-c] Pyradine	19.81	0.069	3%							0.365	3%	0.859	1%	0.811	2%	1.008	0%			
2-Pentadecyn-1-ol	19.86					0.336	0%													
Dodecanal	19.86					0.336	0%													
cis-9,10-Epoxyoxtadecan-1-ol	19.86					0.336	0%													
2-Nonadecanone	20.05					0.223	9%													
2-Undecanone	20.05					0.223	23%													
Dodecanal	20.25	0.085	0%			0.52	6%	0.747	7%	0.62	4%	0.507	5%	0.524	4%	0.673	2%			
Undecanal	20.25	0.085	0%			0.52	10%	0.747	25%	0.62	11%	0.507	14%	0.524	9%	0.673	11%			
9,12,15-Octadecatrienoic Acid, 2-[(trimethylsily)oxy]methyl ethyl ester	20.25			0.126	77%															
2,2-Dimethyl-1-pentamethyldisilamyloxy propane	20.25			0.126	0%															
12-Crown-4	20.4							0.555	0%	0.459	0%	0.495	2%							
Methane, nitroso-	20.4											0.495	0%							
15-Crown-5	20.4							0.555	0%	0.459	0%									
Tetradecane	20.84			0.613	15%															
Decane, 2-methyl	20.84			0.613	1%															
3,4-Dimethyl-isoxazol-5(4H)-one	20.89					0.789	4%	2.871	5%	2.234	5%	3.854	4%	3.639	4%	5.913	4%			
Caprolactam	**20.89**					**0.789**	**34%**	**2.871**	**71%**	**2.234**	**69%**	**3.854**	**81%**	**3.639**	**81%**	**5.913**	**83%**			
1,5,9,9-Tetramethyl-2-methylene-spiro[3.5]non-5-ene	21.18											0.434	4%							
6,8-Nonadiene-2-one, 6-methyl-S-	21.18											0.434	0%							
trans-2-undecenoic acid	21.72							1.187	0%							1.088	0%			

1-Gala-1-ido-octose	21.72																		1.088	0%
1,1,1,3,5,5,7,7,7-Nonamethyl-3-(trimethylsiloxy)tetrasiloxane	21.73	0.406	0%	1.31	1%	0.758	0%			1.032	0%	0.913	0%	0.968	0%				
3-Butoxy-1,1,1,5,5,5-hexamethyl-3 (trimethylsiloxy)trisiloxane	21.73	0.406	0%	1.31	0%	0.758	0%	1.187	0%	1.032	0%	0.913	0%	0.968	0%				
Biphenyl	21.84	0.196	51%	0.278	64%														
Naphthalene, 2-ehtenyl	21.84	0.196	29%	0.278	19%														
1,2-Benzenedicarboxylic acid	21.99					0.324	11%	0.512	28%	0.338	23%	0.404	31%	0.387	28%	0.877	24%		
Phthalic anhydride	21.99					0.324	18%	0.512	48%	0.338	28%	0.404	42%	0.387	42%	0.877	66%		
1-Octadecanesulphonyl chloride	22.28	0.125	0%																
Heptadecane, ,26-dimethyl	22.28	0.125	0%																
Decane, 2-methyl	22.28			0.809	1%														
Hexadecane	22.28			0.809	7%														
Pentdecane	22.28			0.809	8%														
1-iodo-2-methylundecane	22.28	0.125	0%																
1-Octadecanesulphonyl Chloride	22.43			0.164	1%														
Tetracontane, 3,5,24-trimethyl	22.43			0.164	3%														
1-Pentadecene, 2-methyl	22.64	0.1	0%																
3-Trifluoroacetoxytetradecane	22.64	0.1	0%																
4-Trifluoroacetoxytetradecane	22.64	0.1	0%																
10-Heneicosene (c,t)	22.64			0.143	0%														
1-Hexadecanol	22.64			0.143	0%														
Hexadecen-1-ol, trans,9	22.64			0.143	0%														
Pentadecane, 7-methyl	23.01			0.755	26%														

9-methylheptadecane	23.01			0.755	0%															
Pentadecane, 5-methyl	23.11			0.565	7%															
2,6-Dimethyldecane	23.11			0.565	0%															
2,5-Cyclohexadiene-1,4-dione	23.18	1.163	71%	0.644	62%	1.569	59%	4.537	73%	5.883	69%	5.503	74%	5.883	76%	4.277	71%			
2,5-di-tert-Butyl,1,4-benzoquinon	23.18	1.163	4%	0.644	2%	1.569	2%	4.537	4%	5.883	4%	5.503	5%	5.883	5%	4.277	4%			
2-Hexyl-1-octanol	23.31			0.157	0%															
1-Decanol, 2-Hexyl	23.31			0.157	0%															
Dichloroacetic Acid, 2-pentadecyl ester	23.31			0.157	0%															
Ethanone, 1-(2,3,4-trimethylphenyl)-	23.39													0.327	0%					
Ethanone, 1-1-(1,4 - phenylene)bis	23.39													0.327	4%					
Pentadecane 3-methyl	23.46	0.083	0%	0.6	24%															
Hexadecane, 4-methyl	23.46	0.083	0%	0.6	16%															
Sulfurous Acid, butyl tetradecyl est	23.46	0.083	0%																	
10-Heneicosene (c,t)	23.89															1.111	1%			
1-Decanol, 2hexyl	23.89															1.111	2%			
8-Heptadecene	23.89															1.111	1%			
Decane, 2-methyl	23.92			2.622	0%															
Hexadecane	23.93	0.563	15%	2.622	10%															
Dodecane. 2,6,11-trimethyl	23.93	0.563	4%																	
Propanoic Acid, 2-methyl-1-(1,1-dimethylethyl-2-methyl-1,3-propanolyl ester	25.1	0.247	4%	0.597	17%															
Butanoic Acid, Anhydride	25.1	0.247	0%	0.597	0%															
Pentanoic Acid, 2,2,4- trimethyl, -3-carboxy isopropyl, isobutyl ester	25.1			0.597	40%															

Calarene epoxide	26.49									0.534	2%									
2,3-Dihydro-4-Oxo-ionol	26.49									0.534	1%									
2,2,7,7-Tetramethyltricyclo[6.2.1.0(1,6)]undec-4-en-3-one	26.57											0.576	15%							
2,4a-Methanonapthalen-7(4aH)	26.57											0.576	3%							
Naphthalene, 2,2-dimethyl-1-oxa-2-sila-1,2-dihydro-	27.41											0.835	0%							
2-Penten-1-one, 1- (2-hydroxy-5n)	27.41											0.835	3%							
2-(2,6,6-Trimethylcyclohex-1-enyl)cyclopropanecarboxylic acid, methyl ester	27.71									0.58	5%			0.576	5%					
4,4-Dimethyl-3-(3-methylbut-2)	27.71									0.58	0%									
1-(4-Hydroxy-3-isopropenyl-4,7,7-trimethyl-cyclohept-1-enyl)-ethanone	27.71							0.898	3%			0.777	3%							
Acetate, (2,4a,5,8a-tetramethyl-1,2	27.71							0.898	0%			0.777	0%							
5-(7a-Isopropenyl-4,5-dimethyl-)	27.71					0.614	5%													
7a-Isopropenyl-4,5-dimethyloctahydroindene-4-carboxylic acid	27.71					0.614	6%													
2-Butanone, 4-[2-isopropyl-5-methyl-5-(2-methyl-5-oxycyclophenyl) cyclopentyl-	27.7													0.576	0%					
1,3-Dimethyl-5-ethyladamantane	28.7					0.769	0%													
Benzestrol	28.7					0.769	6%													
1,3,5-Trimethyladamantane	28.69							0.978	0%			1.129	0%	0.897	0%					
3-Buten-2-one, 4-(6,6-dimethyl-1-cyclohexen -1-yl)-	28.69							0.978	7%	0.761	7%					1.014	7%			
1,3-Dimethyl-5-ethyladmantane	28.69													0.897	0%					
Oxalic acid, ethyl 2-isopropylphenyl ester	28.69											1.129	2%							
1,4-Methanopthalazine, 1,4,4a,5	28.69									0.761	0%									
1,2-Dimethyl-5-nitroadamantine	28.68															1.014	0%			
p-Anisic acid, 4-nitrophenyl ester	29.06					1.884	0%			2.11	3%	3.071	4%	2.246	0%	2.357	2%			

o-Asnic acid, 4-nitrophenyl ester	29.06					1.884	0%	2.551	0%	2.11	0%										2.357	0%
p-Asnic Acid, 3,4-dichlorophenyl ester	29.06											3.071	3%	2.246	0%							
1-n-Hexyladamantane	29.06							2.551	2%													
o-Asnic acid, 3,4-dichlorophenyl ester	29.06					1.884	0%	2.551	0%	2.11	1%										2.357	0%
2-Ethyl-5-n-propylphenol	29.15					2.113	0%	3.247	1%	2.296	1%	3.548	1%	2.972	1%				3.413	1%		
Spiro-1-(cyclohex-2-ene)-2-(5oxabicyclo[2,1,0]pentane) 1,4,2,6,6-pentamethyl	**29.13**													**2.972**	**20%**		**3.413**	**19%**				
Phenol, 4-(1,1-dimethylpropyl)-	29.15					2.113	13%	3.247	11%	2.296	5%	3.548	22%									
p-Asnic Acid, 3,4-dichlorophenyl ester	29.38					1.57	1%										2.272	2%				
o-Asnic acid, 3,4-dichlorophenyl ester	29.38							2.229	0%	1.758	1%	2.529	0%	2.13	1%		2.272	0%				
o-Asnic acid, 4-nitrophenyl ester	29.38							2.229	0%	1.758	0%	2.529	0%	2.13	1%		2.272	0%				
p-Asnic acid, 4-nitrophenyl ester	29.38					1.57	1%	2.229	4%	1.758	3%	2.529	3%	2.13	6%							
1,3-Cyclohexadiene, 1,2,3,4,5,6-hexamethyl-	29.5					0.699	1%															
Tricyclo(5,4,3,0(1,8)tetradecan-6-	29.5					0.699	10%															
o-Isopropylphenetole	29.51							0.96	4%			1.157	6%									
4-Methyl-2-tert-octylphenol	29.5									0.821	3%			0.969	3%							
Oxalic Acid, ethyl 2-isopropylphenyl ester	29.5							0.96	3%	0.821	1%	1.157	3%	0.969	1%		0.942	1%				
Benzestrol	29.68					1.699	3%	2.303	3%	1.859	2%	2.675	3%	2.124	3%		2.306	3%				
Oxalic acid, ethyl 2-isopropylphenyl ester	29.68					1.699	7%	2.303	15%	1.859	6%	2.675	19%	2.124	7%		2.306	7%				
1-Adamantanecarboxylic acid, 4-chlorophenyl ester	30							1.431	0%	1.079	0%											
Benzestrol	30					0.992	14%			1.079	13%			1.319	11%		1.492	8%				
1-Adamantanecarboxylic acid, 3,4-chlorophenyl ester	30							1.431	0%													
2-Heptanone, 6-methyl-6-[3-methyl]	30					0.992	12%															

Phenol, 4-(1,1-dimethylpropyl)-	30.02														1.69	4%	1.319	9%	1.492	0%		
Phenol;3,5-bis(1-methylethyl)	30.02																1.319	9%				
Adamantane-1-carboxamide-N	30										1.099	0%	1.69	0%								
1,3-Cyclohexadiene, 1,3,5,5,6,6-he	30.25					1.428	6%	2.228	9%													
1-Methyl-3-ethyladamantane	30.25					1.428	0%	2.228	0%	1.438	0%	2.378	0%	1.852	0%							
4-Methyl-2-tert-octylphenol	30.25									1.438	1%			1.852	1%							
Cyclohexane,1,1,4,4 - tetramethyl	30.25					1.428	6%															
o-Asnic acid, 3,4-dichlorophenyl ester	30.46																					
p-Asnic acid, 4-nitrophenyl ester	30.47					2.777	0%	4.313	1%	3.066	1%	4.532	1%	4.188	1%							
p-Asnic acid, 3,4-dichlorophenyl ester	30.47							4.313	0%	3.066	0%	4.532	1%									
1-n-Hexyladamantane	30.47													4.188	1%							
o-Anisic acid, 4-nitrophenyl ester	30.46																					
4-Methyl-2-tert-octylphenol	30.86					0.883	0%	1.339	2%	0.991	0%	1.447	7%	1.301	1%							
1-Methyl-3-ethyladamantane	30.85													1.301	0%							
Adamantane, 1,3-dimethyl-	30.86							1.339	0%	0.991	0%	1.447	1%									
Phenol, 2-methyl-4-(1,1,3,3-tetra)	30.86					0.883	19%															
Ethanol,2-[2-(4-nonylphenoxy)ethyl	38.59											2.486	16%									
2-Propanol, 1-[4-(1,1-dimethylethyl)phenoxy]-	38.62							1.593	0%			2.486	0%									
Benzoic Acid, 2-hydroxy-3-[(hydroxy)]	38.62							1.593	0%													

What opportunities for training and professional development has the project provided?

"Nothing to Report."

How were the results disseminated to communities of interest?

"Nothing to Report."

What do you plan to do during the next reporting period to accomplish the goals?

We will conduct several more cell growth/infection runs to further validate/discover gaseous biomarkers of viral infection. We will conduct GC-MS and THz analyses of gaseous samples collected from cell cultures.

4. **IMPACT:**

What was the impact on the development of the principal discipline(s) of the project?

Our preliminary results, outlined in this report, indicate the possible importance of caprolactam, acetophenone, 1,2 benzisothiazole, 2-butene, 2-methyl-1-butanol, and 2-methyl-propanal as a bio-marker of viral infections. We will further validate this funding. If confirmed the finding will contribute to scientific understanding of viral bio-chemistry. THz sensing technology used in this project will provide capability to track the onset of viral infection.

What was the impact on technology transfer?

"Nothing to Report."

What was the impact on society beyond science and technology?

"Nothing to Report."

5. **CHANGES/PROBLEMS:**

"Nothing to Report"

Changes in approach and reasons for change

"Nothing to Report"

Actual or anticipated problems or delays and actions or plans to resolve them

In Year 2 several cell growth experiments were aborted due to bacterial infection during incubation. We will be taking extra precautions in future experiments to avoid this problem.

Changes that had a significant impact on expenditures

Nothing to report.

Significant changes in use or care of human subjects, vertebrate animals, biohazards, and/or select agents

"Nothing to Report"

Significant changes in use or care of vertebrate animals.

"Nothing to Report"

Significant changes in use of biohazards and/or select agents

"Nothing to Report"

6. **PRODUCTS:**

"Nothing to Report."

7. **PARTICIPANTS & OTHER COLLABORATING ORGANIZATIONS**

What individuals have worked on the project?

- *Provide the following information for: (1) PDs/PIs; and (2) each person who has worked at least one person month per year on the project during the reporting period, regardless of the source of compensation (a person month equals approximately 160 hours of effort). If information is unchanged from a previous submission, provide the name only and indicate "no change."*

Name:	*Ivan Medvedev*
Project Role:	*PI*
Nearest person month worked:	*2*
Contribution to Project:	*Dr. Medvedev's laboratory performs THz analysis of the mixture, lead experimental design for the project. Dr. Medvedev performs overall coordination of the project.*
Funding Support:	

Name:	*Kate Excoffon*
Project Role:	*Co-PI*
Nearest person month worked:	*2*

Contribution to Project:	*Dr. Excoffon' s laboratory is responsible for grows of cell cultures, viral exposure and sample collection. Dr. Excoffon assists Dr. Medvedev in project coordination.*
Funding Support:	

Name:	*Jennifer Martin*
Project Role:	*Co-PI*
Nearest person month worked:	*0*
Contribution to Project:	*Dr. Martin performs GC-MS analyses of gaseous cellular samples.*
Funding Support:	

Name:	*Priyanka Sharma*
Project Role:	*Research Scientist*
Nearest person month worked:	*5*
Contribution to Project:	*Dr. Sharma is responsible for growth of cell cultures.*
Funding Support:	

Name:	*Daniel Tyree*
Project Role:	*Graduate Student*
Nearest person month worked:	*12*
Contribution to Project:	Mr. Tyree is responsible for design of experiments. He is responsible for THz sensing of cellular samples. In coordination with the PI he leads data analysis.
Funding Support:	

Name:	*James Readler*
Project Role:	*Graduate Student*
Nearest person month worked:	*3*
Contribution to Project:	*Mr. Readler is responsible for growth and cell cultures. He assists the PI and Mr. Tyree in design of experimental protocols.*
Funding Support:	NIH/NIAID 1R01AI127816-01A1

Name:	*Hannah Benston*
Project Role:	*Undergraduate Student*
Nearest person month worked:	*1*
Contribution to Project:	*Ms. Benston is assisting Mr. Tyree in performing THz gas sensing and associated data analysis*
Funding Support:	*STTR Phase II, AFOSR FA8650-16-C-6693*

Has there been a change in the active other support of the PD/PI(s) or senior/key personnel since the last reporting period?

NIH/NIAID 1R01AI127816-01A1 (NIH) Excoffon (PI) 9/25/17-8/31/22
"Prevention of adenovirus pathogenesis through downregulation of the apical adenovirus receptor"; The molecular mechanism and anti-adenovirus efficacy of novel molecules that downregulate the expression of the apical adenovirus receptor and adenovirus infection will be investigated in epithelia in vitro and in the cotton rat model for adenovirus pathogenesis in vivo.
Role: PI
No overlap

What other organizations were involved as partners?

"Nothing to Report."